Electronic Supplementary Information (ESI)

Mesoporous N-doped graphene prepared by soft-template method with high performance in Li-S battery

Tianyu Tang,[a] Teng Zhang,[a] Wei Li, [a] Xiaoxiao Huang, [a] Xiaobai Wang, [a] Hailong Qiu, [a] Yanglong Hou*[a]

[a.] Beijing Key Laboratory for Magnetoelectric Materials and Devices (BKLMMD), Beijing Innovation Center for Engineering Science and Advanced Technology (BIC-ESAT), Department of Materials Science and Engineering, College of Engineering, Peking University, Beijing 100871, China. E-mail: hou@pku.edu.cn.

Supplementary Figure

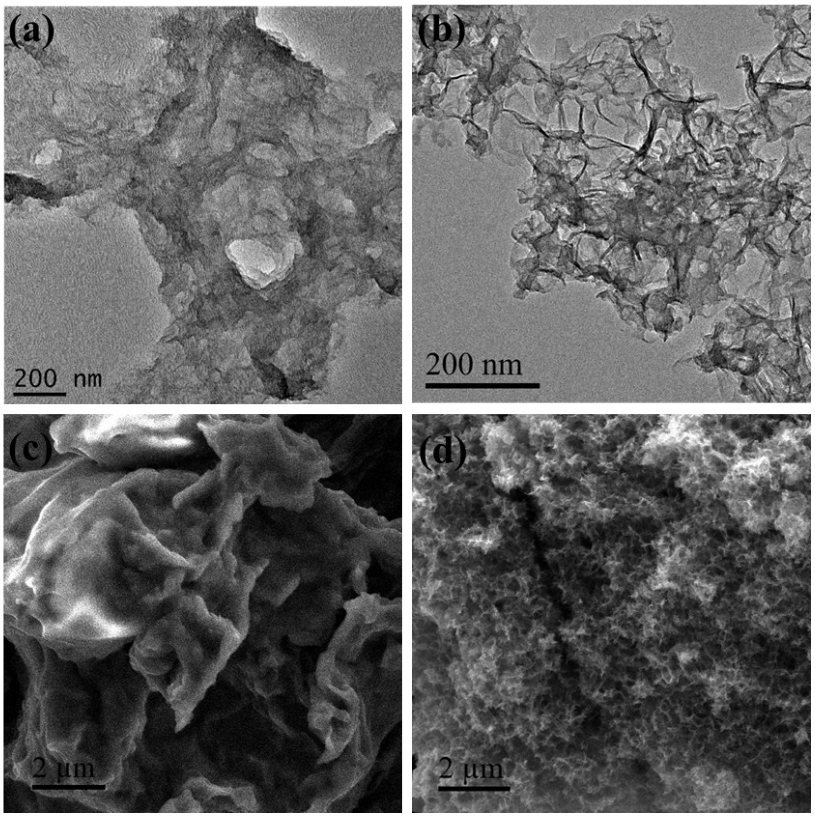

Fig. S1. TEM images of (a) the reduced GO-PF127 composite, (b) NG sheets before annealing. SEM images of (c) the reduced GO-PF127 composite, (d) NG sheets before annealing.

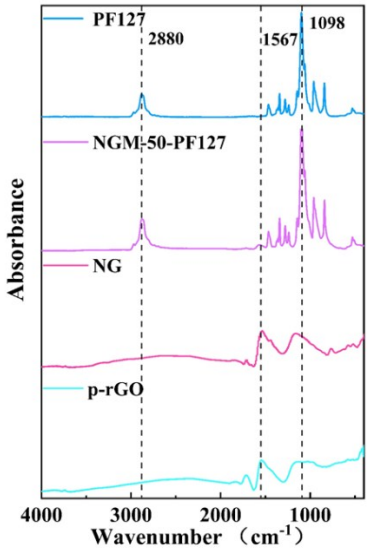

Fig. S2. FT-IR spectra of the p-rGO, NG, NGM-50-PF127 and PF127.

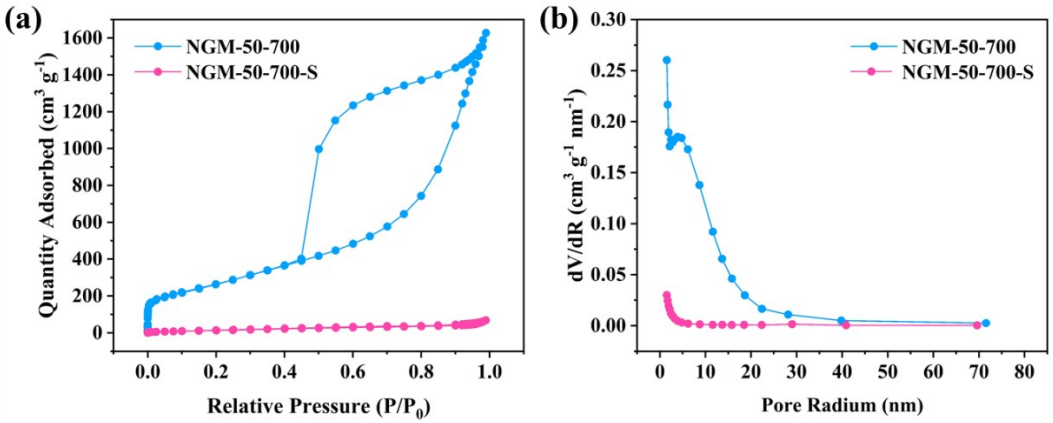

Fig. S3. (a) Nitrogen adsorption−desorption isotherms, and (b) pore size distribution of the NGM-50-700 and NGM-50-700-S.

Sample name	Surface area (m^2/g)	Pore volume (cm^3/g)
p-rGO-700	353.74	1.50
NG-700	563.34	1.64
NGM-50-700	958.72	2.39

Table S1. Brunauer−Emmett−Teller (BET) specific surface area and pore volume of p-rGO-700, NG-700 and NGM-50-700.

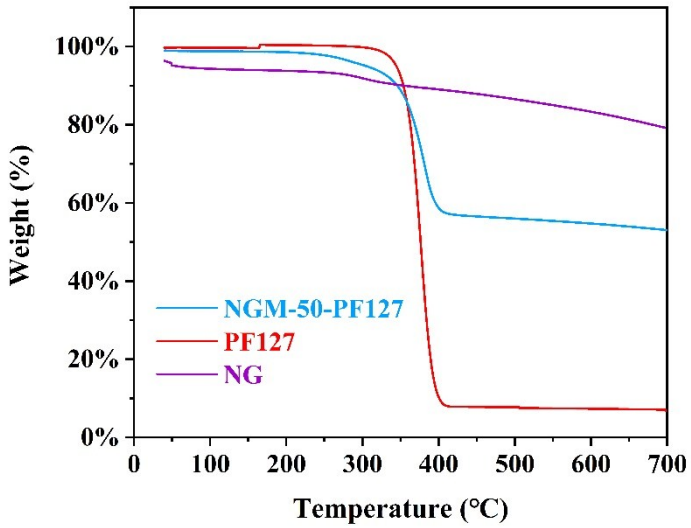

Fig. S4. The thermogravimetric analysis (TGA) of NG, PF127 and NGM-50-PF127.

It can find that the mass loss of NG after TGA test is about 17%. If the mass ratio of NG is x in NGM-50-PF127, 0.17x + 0.93(1-x)=0.47, x=0.61. As a result, the contribution of graphene species to the mass change in TGA test is about 0.61*0.17=0.1037.

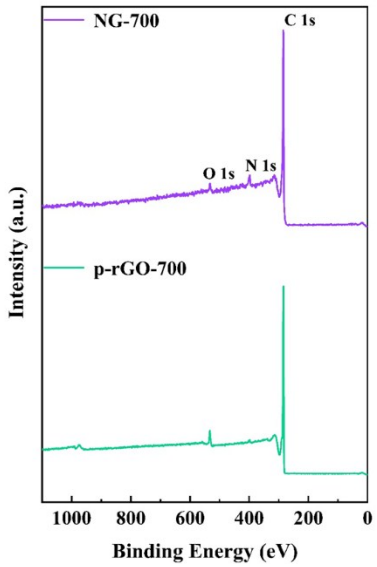

Fig. S5. XPS survey spectrum of p-rGO-700 and NG-700.

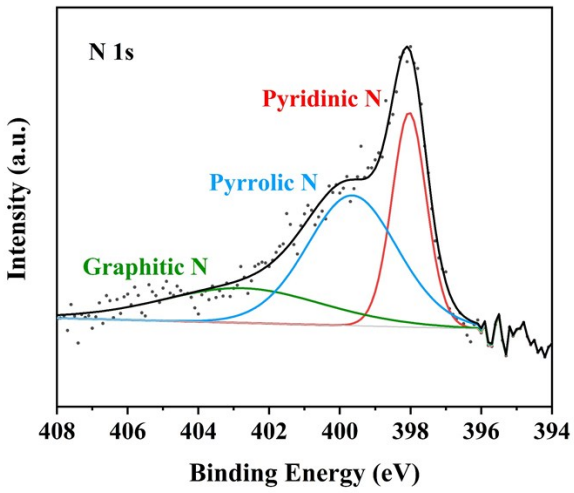

Fig. S6. The high resolution of N 1s spectrum of the NG-700.

Sample name	C (at%)	N (at%)	O (at%)
p-rGO-700	99.07	0.15	0.78
NG-700	95.32	3.51	1.17
NGM-50-700	94.28	4.80	0.92

Table S2. The content of C, N and O in p-rGO-700, NG-700 and NGM-50-700 by XPS.

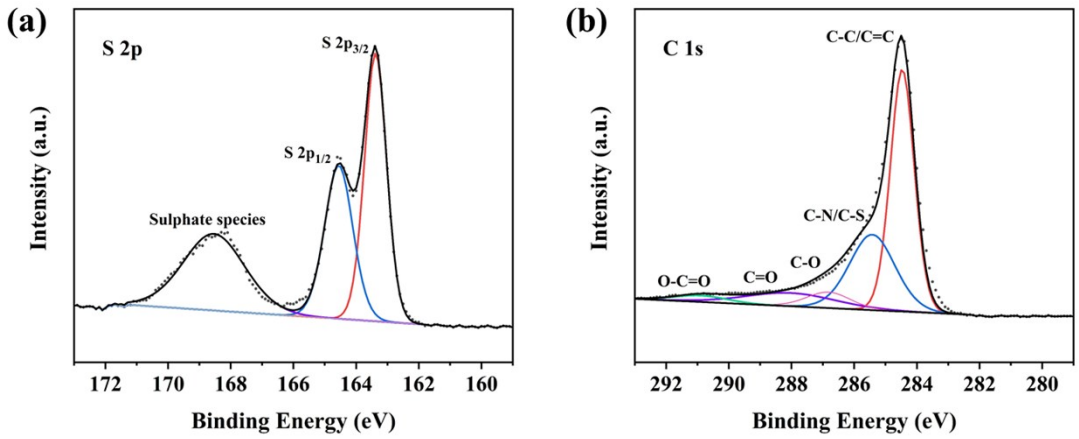

Fig. S7. XPS analysis of NGM-50-700-S (a) S 2p spectrum, (b) C 1s spectrum.

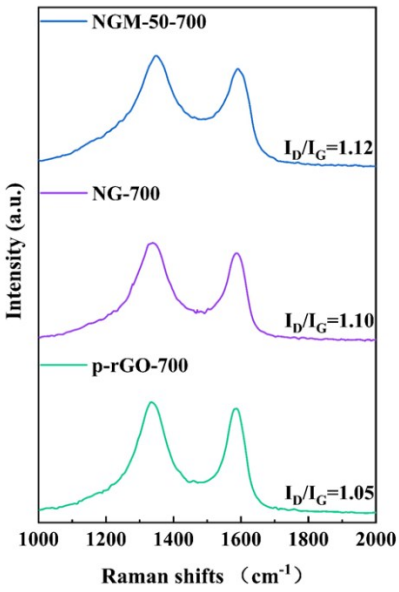

Fig. S8. Raman spectra of the p-rGO-700, NG-700 and NGM-50-700

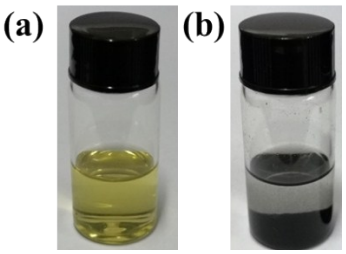

Fig. S9. (a) The lithium polysulfides solution (Li_2S_6), (b) the lithium polysulfides solution (Li_2S_6) containing NGM-50-700 after 12h.

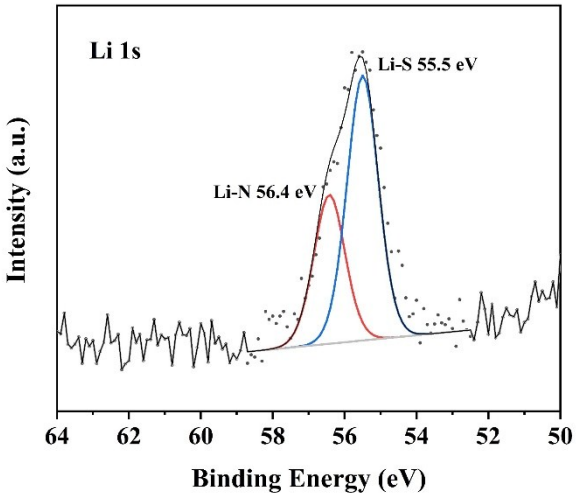

Fig. S10. The high resolution of Li 1s spectrum of the NGM-50-700/Li_2S_6.

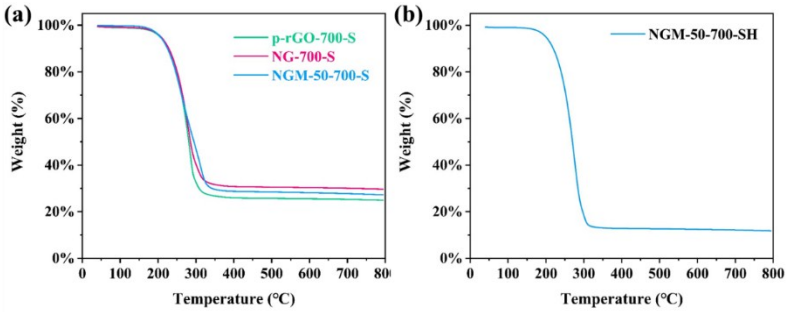

Fig. S11. The sulfur loading of the (a) p-rGO-700-S, NG-700-S, NGM-50-700-S, and (b) NGM-50-700-SH.

Sample name	Sulfur content (wt%)
p-rGO-700-S	74.1
NG-700-S	69.2
NGM-50-700-S	71.2

Table S3. The sulfur content of the p-rGO-700-S, NG-700-S, NGM-50-700-S.

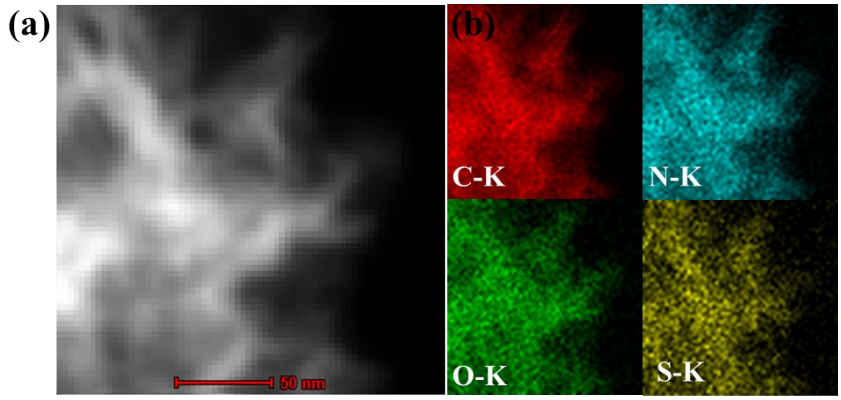

Fig. S12. (a) STEM image of NGM-50-700-S, (b) elemental mapping of NGM-50-700-S.

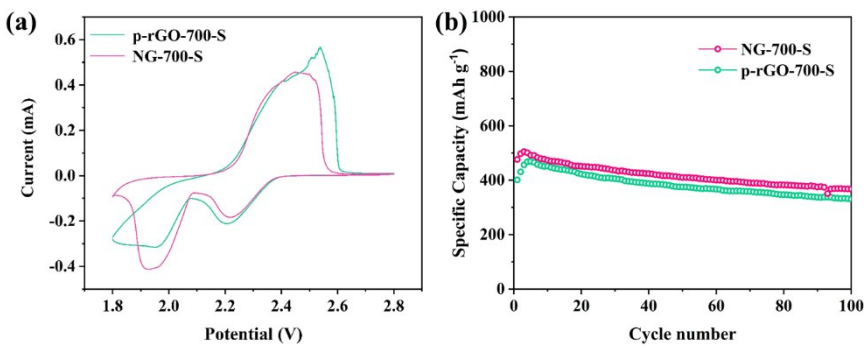

Fig. S13. (a) the CV profile of p-rGO-700-S and NG-700-S at 0.1 mV s^{-1}, (b) cycling performance of p-rGO-700-S and NG-700-S at 0.46 A g^{-1}_{TE}.

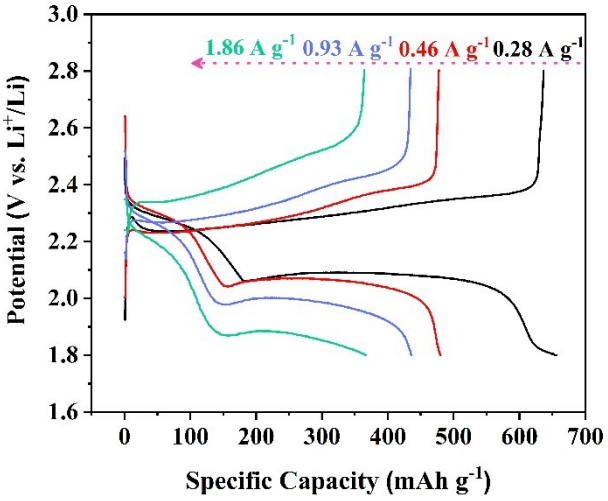

Fig. S14. The voltage profiles of NGM-50-700-S at rates ranging from 0.28 to 1.86 A g^{-1}_{TE}.

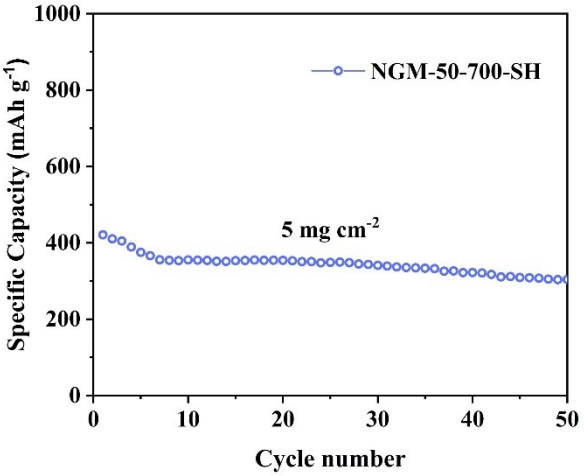

Fig. S15. The cycling performance of NGM-50-700-SH with sulfur loading mass of 5 mg cm^{-2} at 0.81 A g^{-1}_{TE}.

Cathode material	Cathode density	Volumetric capacity	Current density	Cathode energy density (Wh L^{-1})	Reference

	($g\ cm^{-3}$)	($mAh\ cm^{-3}$)	($A\ g^{-1}_{sulfur}$)		
Graphene monolith/S	1.16	401	0.84	852	[1]
3D Al foam/CNT/S	N/A	299	0.17	643	[2]
$NiFe_2O_4$/S	1.33	1282	0.17	~2690	[3]
CNT/S	0.64	668	0.17	~1430	[3]
PCNF/S	N/A	317	0.17	~680	[4]
HDGS/S	1.07	233	0.84	~490	[5]
PVP-hollow S sphere	N/A	375	0.84	~788	[6]
3D NG@S-CNT	0.67	391	0.84	850	[7]
rGO-VS_2/S-64	1.02	350	0.17	~740	[8]
rGO/S-64	0.35	195	0.17	~410	[8]
CNTs–S/300HOPT@G/300HOPT	1.23	498	0.34	~1030	[9]
NGM-S	**0.60**	**356**	**0.84**	**719**	**This work**
	0.96	**503**	**0.84**	**1008**	**This work**

Table S4. Comparison of cathode energy density with several reported works.

References

[1] Li, H.; Tao, Y.; Zhang, C.; Liu, D.; Luo, J.; Fan, W.; Xu, Y.; Li, Y.; You, C.; Pan, Z.-Z.; Ye, M.; Chen, Z.; Dong, Z.; Wang, D.; Kang, F.; Lu, J.; Yang, Q., *Adv. Energy Mater.* **2018,** *8* (18), 1703438.

[2] Cheng, X.-B.; Peng, H.-J.; Huang, J.-Q.; Zhu, L.; Yang, S.-H.; Liu, Y.; Zhang, H.-W.; Zhu, W.; Wei, F.; Zhang, Q.,

J. Power Sources **2014,** *261*, 264-270.

[3] Zhang, Z.; Wu, D.; Zhou, Z.; Li, G.; Liu, S.; Gao, X., *Sci. China Mater.* **2019,** *62* (1), 74-86.

[4] Qie, L.; Manthiram, A., *Adv. Mater.* **2015,** *27* (10), 1694-1700.

[5] Zhang, C.; Liu, D.; Lv, W.; Wang, D.; Wei, W.; Zhou, G.; Wang, S.; Li, F.; Li, B.; Kang, F.; Yang, Q., *Nanoscale* **2015,** *7* (13), 5592-5597.

[6] Li, W.; Zheng, G.; Yang, Y.; Seh, Z. W.; Liu, N.; Cui, Y., *Proc. Natl. Acad. Sci. U. S. A.* **2013,** *110* (18), 7148-7153.

[7] Zhai, P.; Huang, J.; Zhu, L.; Shi, J.; Zhu, W.; Zhang, Q., *Carbon* **2017,** *111*, 493-501.

[8] Cheng, Z.; Xiao, Z.; Pan, H.; Wang, S.; Wang, R., *Adv. Energy Mater.* **2018,** *8* (10), 1702337.

[9] Xiao, Z.; Yang, Z.; Zhou, L.; Zhang, L.; Wang, R., *ACS Appl. Mater. Interfaces* **2017,** *9* (22), 18845-18855.